Investigation of layer interface model of multi-layer structure using semi-analytical and FEM analysis for eddy current pulsed thermography

Qiuji Yi
School of Engineering, Newcastle University, Merz Court, NE1 7RU,
Newcastle upon Tyne, UK
Qiuji.yi@newcastle.ac.uk

GuiYun Tian
School of Engineering, Newcastle University, Merz Court, NE1 7RU,
Newcastle upon Tyne, UK
g.y.tian@newcastle.ac.uk

Houssem Chebbi
CEA LIST, Laboratoire de Simulation et de Modlisation en Electromagntisme,
Gif-sur-Yvette, 91191, France.
Houssem.CHEBBI@cea.fr

Denis Prémel
CEA LIST, Laboratoire de Simulation et de Modlisation en Electromagntisme,
Gif-sur-Yvette, 91191, France.
Denis.PREMEL@cea.fr

Abstract— The use of a multi-layer structure is widely recognized in aerospace engineering due to the fact that structural and functional properties can be implemented by designing geometric structure. Eddy current pulsed thermography (ECPT) is one of the crucial NDT techniques to inspect and evaluate the defects in composite multi-layer structure due to the volumetric heating nature. Thus, it is important to investigate the scattering electromagnetic wave into the interface of multi-layer structure to improve the detectability and evaluation capbility of an ECPT system. In this work, the conductivity tensor form is used to describe the scattering EM wave in the 3D FEM model to investigate the fiber orientation influence on each layer interface. The semi-analytical model is used to prove the concept and both results are validated by experimental studies with dedicated samples. The findings can be applied for simulating the scattering electromagnetic behavior in the interface of the multi-layer structure.

Keywords— layer interface model, multi-layer structure, eddy current, 3D finite element model, semi-analytical model

I Introduction

The use of CFRP materials has become increasingly popular among conventional engineered materials due to their extraordinary mechanical and thermal properties, such as high strength-to-weight ratio, corrosion resistance, improved fatigue performance and low coefficient of thermal expansion. Multilayer composites are a broad and important group of structural and functional materials whose properties may vary over a very wide range. The possibility of combining in one monolithic material layers of a different nature that exhibit markedly different physical properties makes it possible to construct materials for very different functional purposes, including impact and high temperature, heat and corrosion-resistance, heat-conducting, and heat-protective.

Eddy Current Pulsed Thermography (ECPT) has been recently proposed for multi-layer composite structure evaluation. When ECPT is applied to CFRP, the stimulation can be considered volumetric since the electrical conductivity is relatively low. Depending on the excitation frequency of the Eddy Current (EC) and the sample thickness, the typically achieved skin depths are greater than the sample thickness itself, or at least comparable to it [1]. In addition, due to the multi-physics nature of the ECT, the electrical and thermal properties can be evaluated simultaneously in one experiment. ECT is also less influenced by the surface conditions of the SUT such as emissivity, roughness, etc. [2]. Moreover, ECT can be exploited to evaluate the barely visible impact damage on composites [3] and the presence of delamination [4, 5].

In order to understand the electromagnetic and thermal behaviour of the induction thermography. Simulation and modelling are needed. The current challenges for modelling inductive thermography are the anisotropic conductivity of the material especially the through-thickness electrical conductivity [6]. The electrical conductivity of CFRPs depends strongly on the orientation of carbon fibers: the longitudinal conductivity (parallel to the fiber direction, σ_L) is the highest; while the transverse conductivity (perpendicular to the fibers, σ_T) is relatively lower and on the same order of magnitude as the electrical conductivity along the thickness of the specimen (σ_{Th})[6]. Additionally, this anisotropic electrical conductivity is further compounded by a strong dependence on the presence of interfaces between adjacent plies. These interfaces vary in size, physical composition, and chemical composition and therefore result in uncertain value [7]. In addition, σ_{Th} (according to the thickness of CFRP laminates) can be greatly affected by the presence of interfaces between layers and the lamination of the individual plies. For instance, the stacking sequence tends to increase the dispersion of measurements [8]. Thus, using σ_{Th} to interpret the interface condition of the laminated composites can be the solution to model the anisotropic behaviour of the composites.

Due to the important number of carbon fibers impregnated in each layer, it is very difficult to take into account the real geometry in the simulation. The composite layer is then replaced by a homogenized one [9]. Moreover, as the composite sheets have a small thickness compared with their other dimensions, shell elements can be used to reduce the number of unknowns. The case of three-dimensional (3-D) induction heating simulation of composite plate with equivalent anisotropic conductivities has been presented [10]. In the meantime, CEA LIST has recently developed a new semi-analytical method for the computation of the 3D primary fields induced by an eddy current probe in a homogeneous conductor presenting a local perturbation of the geometry [11]. This approach is an extension of the curvilinear coordinate method (CCM), which is efficient for the computation of the fields scattered by 2D diffraction gratings enlightened by a plane wave or perfectly conductive random surfaces [12, 13].

978-1-7281-4460-3/20/$31.00 ©2020 IEEE

In this work, 3-D induction heating simulation model of a multilayer anisotropic composite materials is proposed. The real geometry of multilayer composite materials with an equivalent anisotropic individual layer is considered. A global equivalent model is then introduced to consider the different fibbers' orientations. In addition, to model the scattering electromagnetic field penetrating which contains the internal reflections occurring inside every layer composing the structure, the conductivity tensor in perpendicular direction in FEM model is obtained by approximating the output of semi-analytical method.

The rest of the paper is organized as follows: Section II introduces the methodology of FEM model and semi-analytical method to simulate the electromagnetic behaviour of CFRP. Section III presents the experimental setup. Section IV gives the results and analysis and conclusion is introduced in Section V.

II LAYER INTERFACE MODELLING

3D FEM method and semi-analytical models are introduced and discussed.

A 3D FEM method for multi-layer CFRP

To model the anisotropic behaviour of composites material, the electrical and thermal conductivities (σ_i, λ_i) have tensor form as follows [10]:

$$\sigma_i = \begin{bmatrix} \sigma_{xx_i} & \sigma_{xy_i} & 0 \\ \sigma_{yx_i} & \sigma_{yy_i} & 0 \\ 0 & 0 & \sigma_{z_i} \end{bmatrix} \quad (1)$$

$$\lambda_i = \begin{bmatrix} \lambda_{xx_i} & \lambda_{xy_i} & 0 \\ \lambda_{yx_i} & \lambda_{yy_i} & 0 \\ 0 & 0 & \lambda_{z_i} \end{bmatrix} \quad (2)$$

This work considers the conductivity tensor to represent electromagnetic properties of each laminate. The relationship between conductivity tensor and the orientation of the layer is shown in Eq. (3) and (4) respectively.

$$\sigma_\theta = \begin{bmatrix} \sigma_L\cos^2\theta + \sigma_T\sin^2\theta & \frac{\sigma_L - \sigma_T}{2}\sin 2\theta & 0 \\ \frac{\sigma_L - \sigma_T}{2}\sin 2\theta & \sigma_L\cos^2\theta + \sigma_T\sin^2\theta & 0 \\ 0 & 0 & \sigma_{Th} \end{bmatrix} \quad (3)$$

$$\lambda_\theta = \begin{bmatrix} \lambda_L\cos^2\theta + \lambda_T\sin^2\theta & \frac{\lambda_L - \lambda_T}{2}\sin 2\theta & 0 \\ \frac{\lambda_L - \lambda_T}{2}\sin 2\theta & \lambda_L\cos^2\theta + \lambda_T\sin^2\theta & 0 \\ 0 & 0 & \lambda_{Th} \end{bmatrix} \quad (4)$$

For N layers of laminated composites, each layer i 's magnetic field can be calculated:

$$\begin{cases} \frac{d^2H_x(z)}{dz^2} - j\omega\mu \cdot \sigma_{yy_i}H_x(z) = j\omega\mu \cdot \sigma_{yx_i}H_y(z) \\ \frac{d^2H_y(z)}{dz^2} - j\omega\mu \cdot \sigma_{xx_i}H_y(z) = j\omega\mu \cdot \sigma_{xy_i}H_x(z) \\ \frac{d^2H_z(z)}{dz^2} - j\omega\mu \cdot \sigma_{z_i}H_z(z) = 0 \end{cases} \quad (5)$$

The boundary conditions of the magnetic field are as follows:

$$\begin{cases} H\left(\frac{p_i}{2}\right) = H_i \\ H\left(-\frac{p_i}{2}\right) = H_{i+1} \end{cases} \quad (6)$$

where $p_i$represents the thickness of layer i.

According to Faraday's law combined with the local form of Ohm's law, the anisotropic electrical field of each layer can be obtained as follows:

$$\begin{pmatrix} E_i \\ E_{i+1} \end{pmatrix} = k \times \begin{pmatrix} \alpha_i & -\beta_i \\ \beta_i & -\alpha_i \end{pmatrix} \begin{pmatrix} H_i \\ H_{i+1} \end{pmatrix} \quad (7)$$

Where k is the normal vector and α_i, β_i are scalar values dependable on electrical conductivity tensor is shown in Eq (1) and can be calculated as [14].

After obtaining current density E_i of layer i. The heat source Q_i of in layer i can be obtained as:

$$Q_i = J_i^T \cdot E_i = J_i^T \cdot \sigma_i^{-1} \cdot J_i \quad (8)$$

$$J_i = \mathrm{rot}H(i) \quad (9)$$

After the calculation of Q_i of each layer. The heat transfer inside the anisotropic material can be solved as:

$$\rho_i C_{p_i} \frac{\partial T}{\partial t} + \mathrm{div}(-\lambda_i \cdot \mathrm{grad}T) = Q_i \quad (10)$$

with the boundary condition:

$$-\lambda_i \cdot \frac{\partial T}{\partial t} = h(T - T_a) \quad (11)$$

Where λ_i is the tensor form shown in Eq. (2), ρ_i is the material density, C_{p_i} is the specific heat, h is the convective coefficient, T is the temperature of layer i and T_a is the room temperature.

For all cases, the 3-D electromagnetic and thermal behaviour are solved in COMSOL multi-physics.

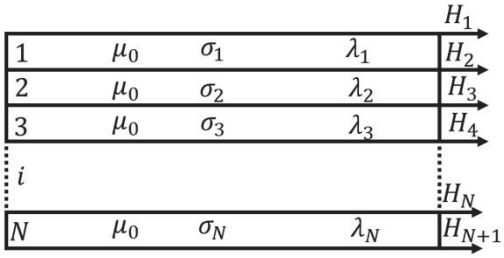

Fig 1. Multi-layer representation by FEM.

B Semi-analytical method

The configuration for the semi-analytical method in this paper is shown in Fig.2. It consists of a multilayer stack with N layers, labelled by p=1,2,...,N of the wave number k_{cp} and thickness e_p. each layer is bounded by the p^{th} and $(p+1)^{th}$ interfaces in which the eigenmodes are denoted by $\Psi_p^{\pm}$. At the p^{th} interface, we have the outgoing waves corresponding to the coefficients (a_p^{+up}, a_p^{-dn}) and the incoming waves corresponding to the coefficients (a_p^{-up}, a_p^{+dn}) .The superscripts - and + refers to transmission and reflection respectively. Moreover, the superscripts (up) and (dn) refer to the upper and downer coefficients regarding the p^{th} interface. Assuming that the 0^{th} and the Nth layers are in air, results from the incident field due to the coil and $a_N^+ = 0$ Thus, the 2D discrete FT along Ox and Oy was adopted:

$$F(\alpha, \beta, z) = \sum_{u=-M_u}^{u=M_u} \sum_{v=-M_v}^{v=M_v} F(x, y, z) e^{-i\alpha_u x} e^{-i\beta_v y} \quad (12)$$

Where

$$\begin{cases} \alpha_u = \frac{2\pi u}{dx}, -M_u < u < M_u \\ \beta_v = \frac{2\pi v}{dy}, -M_v < v < M_v \end{cases} \quad (13)$$

Therefore, the partial derivatives $(\partial_i = \frac{\partial}{\partial_i})$ become $\partial_x \equiv -i\alpha$ and $\partial_y \equiv -i\beta$. We take also the assumption of variable separation: $f(x,y,z) = f(x,y)e^{-iyz}$ so $\partial_z \equiv -i\gamma$. The modal representation of the field depends on the truncation orders M_u and M_v of the FT. Numerically, each component is a matrix of dimension L, with $L = (2M_u + 1)(2M_v + 1)$. Depending on the nature of the considered anisotropic layer, the modal decomposition is presented in [12].

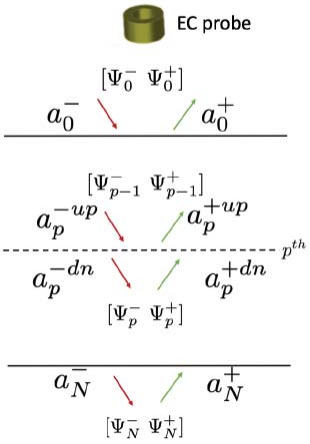

Fig. 2. General diagram: multi-layered structure simulation using semi-analytical model

III EXPERIMENTAL SETUP AND STUDIES

To validate two simulation approaches, experiments on two-layer thin CFRP plate are conducted. As fig. 3(c) shows, the ECPT contains four units, an excitation module with a rectangle coil, an infrared camera, a signal generator, and a computer. In this study, only the operational RMS current and frequency of the excitation module were changed to 300 A and 300 kHz, respectively.The heating induced by eddy current is 500 ms. A 10 mm lift-off between the coil's bottom edge and the top faces of the specimen was kept in all the ROIs' testing. In addition, as shown in fig 3(a) and fig 3(b), the 0-45 sequence sample is used for the experiment. The parameters for the sample are shown in Table I.

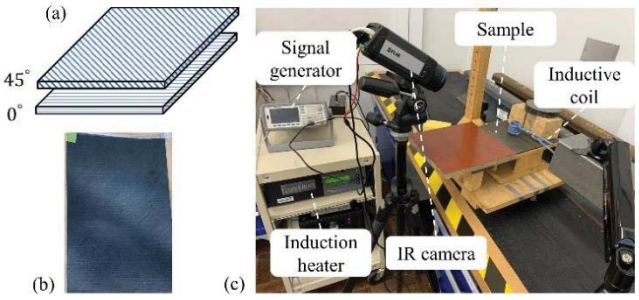

Fig 3 experimental details: (a) sample sketch, (b) sample picture ,(c) experimental setup

Table I: Sample parameters

Parameters	Value	Unit
Relative permeability	1	1
Electrical conductivity(fibre axis,$\sigma_L, \sigma_T, \sigma_{th}$)	{39000,7.9,7.9}	S/m
Relative permittivity	4.3	1
Thermal conductivity(fibre axis,$\lambda_L, \lambda_T, \lambda_{th}$)	{60, 4, 4}	W/(m·K)
Density	1500	kg/m³
Heat capacity at constant pressure	1000	J/(kg·K)

IV RESULTS AND ANALYSIS

In order to validate the proposed FEM model, the temperature evolution over time is compared for experimental and simulated data. It is observed that in Fig 4, the experimental data are scattering around the simulated data, which confirms the validation of FEM data and experimental data.

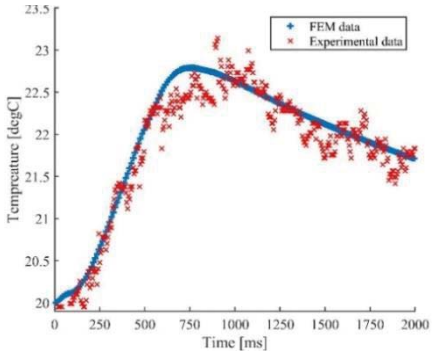

Fig 4 Transient temperature validation of FEM model and experimental

After the validation of the model, the semi-analytical model is calculated based on the parameters of the FEM model. The eddy current density distribution of the top layer and bottom layer are shown in Fig 5 and Fig 6. The quantitative analysis on the amplitude and distribution of eddy current intensity and thermal transient patterns are compared. It is observed that when σ_{th} is equal to 8[S/m] in both cases, the magnitude in FEM Fig 5 and Fig 6 is slightly higher than that of semi-analytical model. The behavior is also observed in Figs 7(a) and 10(a). To simulate the behavior of scattering electromagnetic field, smaller value is applied to approximate the results of semi-analytical model. Thus, it is observed that in Fig 8 and Fig 9 that the amplitude of FEM model and semi-analytical model was approximated in terms of using 2[S/m] as σ_{Th}. Data of one line in Fig 8 and Fig 9 were extracted as shown in Fig 7(b) and Fig 9(b) to prove that using 2[S/m] as σ_{Th} can help describe the scattering of electromagnetic field in FEM.

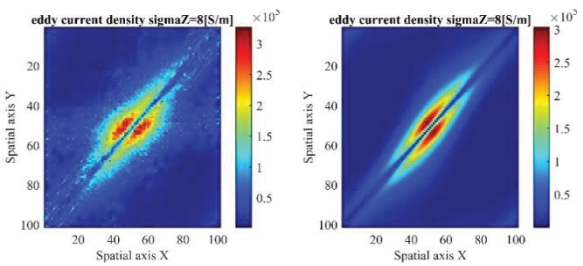

(a) (b)

Fig5 Comparison of Eddy current density distribution on the top surface (45° fibre orientation) (a) FEM model σ_{Th} = 8 S/m ,(b) Semi-analytical model σ_{Th} = 8 S/m

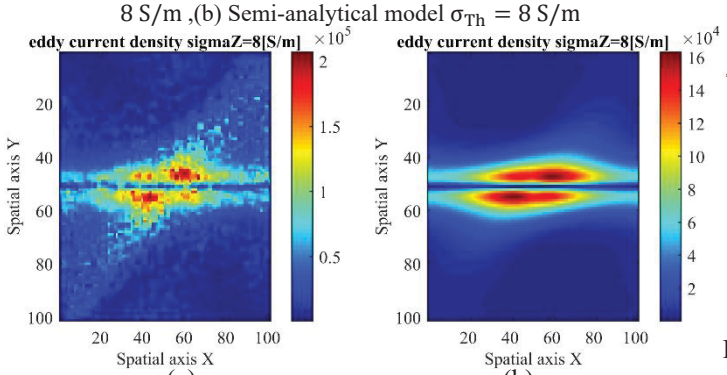

(a) (b)

Fig6 Comparison of Eddy current density distribution on the bottom surface(0° fibre orientation) (a) FEM model σ_{Th} = 8 S/m ,(b) Semi-analytical model σ_{Th} = 8 S/m

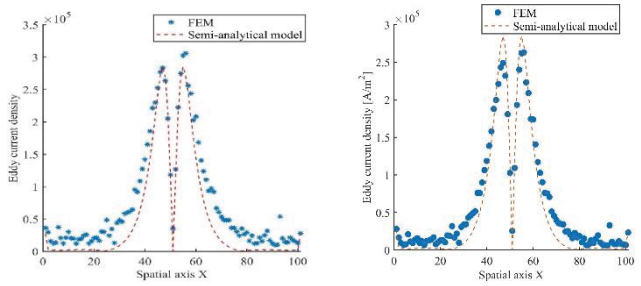

(a) (b)

Fig7 Comparison of top surface cross section eddy current density (when Spatial axis Y=50) of FEM and semi-analytical calculation: (a) FEM model σ_{Th} = 8 S/m ,Semi-analytical model σ_{Th} = 8 S/m ,(b) FEM model σ_{Th} = 2 S/m ,Semi-analytical model σ_{Th} = 8 S/m

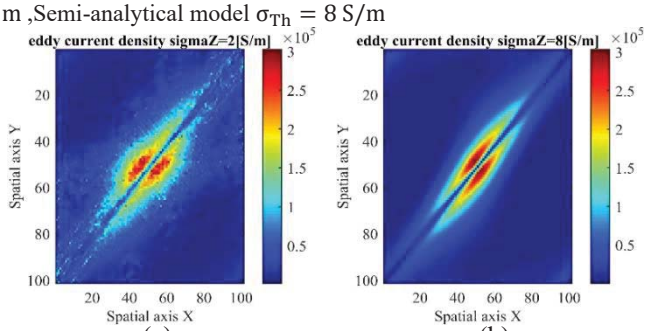

(a) (b)

Fig8 Comparison of Eddy current density distribution on the top surface (45° fibre orientation) (a) FEM model σ_{Th} = 2 S/m ,(b) Semi-analytical model σ_{Th} = 8 S/m

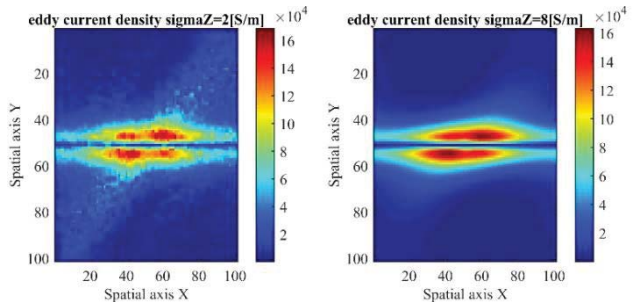

Fig9 Comparison of Eddy current density distribution on the top surface (0° fibre orientation) (a) FEM model σ_{Th} = 2 S/m,(b) Semi-analytical model σ_{Th} = 8 S/m

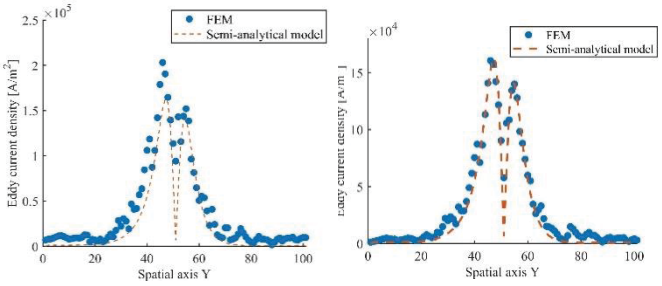

(a) (b)

Fig10 Comparison of bottom surface cross section eddy current density (when Spatial axis X=60) of FEM and semi-analytical calculation: (a) FEM model σ_{Th} = 8 S/m ,Semi-analytical model σ_{Th} = 8 S/m ,(b) FEM model σ_{Th} = 2 S/m , Semi-analytical model σ_{Th} = 8 S/m

V CONCLUSION AND FUTURE WORK

Based on the above analysis, the conclusions are as follows:

1.The scattering electromagnetic field at the interface in multi-layer structure is modelled by the semi-analytical model and the results are used to model the interface in FEM methods.

2.Experimental results for ECPT match with the simulated study. However, it is observed that temperature experimental data at heating stage is slightly lower than simulated output, which can be due to the lack of description of the scattering electromagnetic field in FEM.

3.The scattering EM field in the interface can be modelled by varying the through-thickness conductivity, which is proved in this work.

Future work will continue to investigate the relationship between σ_{Th} and different stacking sequences of the composite material

ACKNOWLEDGEMENT

This project is funded by the European Union's Horizon 2020 research and innovation programme under the Marie Skłodowska-Curie grant agreement No 722134 – NDTonAIR.

REFERENCE:

[1] Yang R, He Y. Eddy current pulsed phase thermography considering volumetric induction heating for delamination evaluation in carbon fiber reinforced polymers. Applied Physics Letters. 2015;106:234103.

[2] Zhu J, Min Q, Wu J, Tian GY. Probability of detection for eddy current pulsed thermography of angular defect quantification. IEEE Transactions on Industrial Informatics. 2018;14:5658-66.

[3] Liang T, Ren W, Tian GY, Elradi M, Gao Y. Low energy impact damage detection in CFRP using eddy current pulsed thermography. Composite Structures. 2016;143:352-61.

[4] Yi Q, Tian G, Malekmohammadi H, Zhu J, Laureti S, Ricci M. New features for delamination depth evaluation in carbon fiber reinforced plastic materials using eddy current pulse-compression thermography. NDT & E International. 2019;102:264-73.

[5] Yi Q, Tian G, Yilmaz B, Malekmohammadi H, Laureti S, Ricci M, et al. Evaluation of debonding in CFRP-epoxy adhesive single-lap joints using eddy current pulse-compression thermography. Composites Part B: Engineering. 2019;178:107461.
[6] Lin Y, Gigliotti M, Lafarie-Frenot MC, Bai J, Marchand D, Mellier D. Experimental study to assess the effect of carbon nanotube addition on the through-thickness electrical conductivity of CFRP laminates for aircraft applications. Composites Part B: Engineering. 2015;76:31-7.
[7] Selvakumaran L, Lubineau G. Electrical behavior of laminated composites with intralaminar degradation: a comprehensive micro-meso homogenization procedure. Composite Structures. 2014;109:178-88.
[8] Barakati A, Zhupanska O. Mechanical response of electrically conductive laminated composite plates in the presence of an electromagnetic field. Composite Structures. 2014;113:298-307.
[9] Senghor FD, Wasselynck G, Bui HK, Branchu S, Trichet D, Berthiau G. Electrical conductivity tensor modeling of stratified woven-fabric carbon fiber reinforced polymer composite materials. IEEE Transactions on Magnetics. 2017;53:1-4.
[10] Bui HK, Wasselynck G, Trichet D, Ramdane B, Berthiau G, Fouladgar J. 3-D modeling of thermo inductive non destructive testing method applied to multilayer composite. IEEE Transactions on Magnetics. 2013;49:1949-52.
[11] Caire F, Prémel D, Granet G. Fast computation of the fields diffracted by a multi-layered conductor with non-parallel rough interfaces. Application to eddy-current non-destructive testing simulation. IEEE Transactions on Magnetics. 2015;51:1-4.
[12] Prémel D, Granet G. Development of the curvilinear coordinate method for the computation of quasi-static fields induced by an eddy current probe scanning a 3D conductor of complex shape characterized by an arbitrary 2D surface. International Journal of Numerical Modelling: Electronic Networks, Devices and Fields. 2018;31:e2219.
[13] Prémel D, Granet G. Fast computation of the response of any 3D Eddy Current probe scanning a 3D stratified conductor characterized by a set of arbitrary interfaces of complex shape. International Journal of Applied Electromagnetics and Mechanics. 2019:1-7.
[14] Ramdane B, Trichet D, Belkadi M, Saidi T, Fouladgar J. Electromagnetic and thermal modeling of composite materials using multilayer shell elements. IEEE Transactions on Magnetics. 2010;47:1134-7.